Huge Instability of Pt/C Catalysts in Alkaline Medium

Anicet Zadick, Laetitia Dubau, Nicolas Sergent, Grégory Berthomé, Marian Chatenet

Huge instability of Pt/C catalysts in alkaline medium

Anicet Zadick [‡,a,b,*], Laetitia Dubau [‡,a,b], Nicolas Sergent [a,b], Grégory Berthomé [c,d], Marian Chatenet [‡,a,b,e,*]

[a] University Grenoble Alpes, LEPMI, F-38000 Grenoble, France

[b] CNRS, LEPMI, F-38000 Grenoble, France

[c] University Grenoble Alpes, SIMAP, F-38000 Grenoble, France

[d] CNRS, SIMAP, F-38000 Grenoble, France

[e] French University Institute (IUF), Paris, France

ABSTRACT: The stability of carbon-supported electrocatalysts has been largely investigated in acidic electrolytes, but the literature is much scarcer regarding similar stability studies in alkaline medium. Herein, the degradation of Vulcan XC-72-supported platinum nanoparticles (noted Pt/C), a state-of-the-art proton-exchange membrane fuel cell electrocatalyst, is investigated in alkaline medium by combining electrochemical measurements and identical-location transmission electron microscopy (ILTEM); electrochemical surface area (ECSA) losses were bridged to electrocatalyst morphological changes. The results demonstrate that the degradation in 0.1 M NaOH at 25°C is severe (60 % of ECSA loss after only 150 cycles between 0.1 and 1.23 V *vs*. RHE), which is about 3 times worse than in acidic media for this soft accelerated stress test (AST). Severe carbon corrosion has been ruled out according to Raman spectroscopy and X-ray photoelectron spectroscopy (XPS) measurements and it seems that the chemistry of the carbon support, and in particular the interface (chemical bounding) between the Pt nanoparticles and their carbon substrate, does play a significant role in the observed degradations.

KEYWORDS. Alkaline electrolytes; Carbon-supported platinum nanoparticles (Pt/C); High surface area carbon; Durability; Identical-location transmission electron microscopy (ILTEM); Raman spectroscopy.

1. Introduction

Platinum (and platinum alloy) nanoparticles supported onto high-surface area carbon – a cheap, easily structured and conductive material – are the state-of-the-art electrocatalyst for fuel cell applications [1,2]. It is no secret that these materials undergo severe degradations at the cathode of proton exchange membrane fuel cells [3-5]; as such Pt/C degradations have been massively investigated at high potential values (above 0.6 V *vs.* RHE) and in acidic media, especially for oxygen reduction reaction (ORR) [6-9]. On the contrary, almost no studies have been conducted for an application as electrode material in (direct) alkaline fuel cells (*i.e.* in alkaline media), except investigations at bulk platinum (and bulk gold) surfaces [10]. Herein, the stability of a state-of-the-art Pt/C electrocatalyst is compared in alkaline and in acidic media by correlating the results of electrochemical characterizations, Identical-Location Transmission Electron Microscopy (ILTEM) imaging and physicochemical analyses (Raman spectroscopy and X-ray photoelectron spectroscopy, XPS).

2. Experimental Section

The Pt/C catalyst was purchased from E-Tek® (20% weight fraction, Vulcan XC72 carbon black substrate) and used as-received without any further treatment. A catalyst ink was prepared by mixing 10 mg of catalyst powder, 7.74 mL of MQ-grade water (18.2 MΩ cm, < 3 ppb Total Organic Carbon, Elix + Milli-Q Gradient, Millipore), 18.3 µL of 5 wt. % Nafion® solution (Electrochem. Inc.®) and 33.9 µL of isopropanol; after 30 min ultrasonic stirring before each experiment, 10 µL of this ink were deposited on a 5 mm-diameter glassy-carbon electrode (13.07 μg_{Pt} cm^{-2} cover the electrode surface), previously polished until 1 µm with diamond paste and copiously rinsed in acetone, ethanol and water, respectively.

The accelerated stress tests (AST) have been performed in 0.1 M solution of H_2SO_4, $HClO_4$ and NaOH; the high-purity reagents were all provided from Merck (Suprapur quality) and the electrolytic solutions were prepared using MQ-grade water.

All the experiments were performed at 25°C, under argon atmosphere (1 atm), using a VSP (Bio-Logic®) potentiostat in a three-electrode cell. The counter-electrode was a carbon

plate – to avoid the dissolution and the redeposition of the counter-electrode material on the working electrode – and the reference electrode was either an aqueous mercury sulfate electrode (MSE: $Hg|Hg_2SO_4|K_2SO_4$, saturated) for acidic media, or a freshly-prepared reversible hydrogen electrode (RHE) for experiments in alkaline solution. A new RHE was prepared every 2 hours of experiments to avoid any bias in the reference potential value; all potential values (even for acidic media) are expressed on the RHE scale.

As stated in the introduction, this paper intends to study whether alkaline media are more aggressive (or not) than acidic ones towards state-of-the-art fuel cell electrocatalysts. The present work was performed in the frame of a larger study which is devoted to the oxidation of complex non-carbon fuels of the borohydride and nitrogen families ($NaBH_4$, NH_3BH_3, $N_2H_4BH_3$) [11-13], and it was firstly chosen to perform experiments in pure NaOH to verify how this solution impacts the Pt/C morphology. Therefore, the potential domain studied corresponds to that useful for the characterization of these fuels oxidation. As such, the AST consists of 150 cycles between 0.1 and 1.23 V *vs.* RHE at 100 mV sec^{-1} in the electrolyte solution (0.1 M of H_2SO_4, $HClO_4$ or NaOH). Each AST precedes and is preceded by two measurements: i) 15 cycles in 0.1 M H_2SO_4 (50 mV sec^{-1}, between 0.1 and 1.33 V *vs.* RHE) called *Characterization test* (Fig.1.a,c,e,g) and then ii) a *CO-stripping test* (6 min CO adsorption followed by 39 min Ar purge at 0.15 V *vs*. RHE, followed by 3 cycles in 0.1 M H_2SO_4, 20 mV sec^{-1}, between 0.1 and 1.33 V *vs.* RHE; Fig.1.b,d,f). The CO-stripping voltammograms were used to measure the ECSA of the Pt/C electrocatalysts prior/after each AST, and the corresponding values enabled to calculate the relative ECSA losses upon each AST.

The results are then compared and correlated to ILTEM data, where each AST was reproduced directly on TEM grids (Gold + Lacey Carbon), and the same regions were observed before and after the degradation test. The TEM micrographs were obtained on a JEOL 2010 TEM apparatus, equipped with a LaB_6 filament operating at 200 kV (point to point resolution 0.19 Å), and used to build particle-size distribution (PSD) histograms (*ca.* more than 400 isolated nanoparticles being counted for statistical relevance) on Fig.2.e,h,k. As in Ref. [14], it was chosen to count the Pt nanoparticles exactly in the same regions before and after the AST, to evaluate in a quantitative manner the nanoparticles loss upon each AST.

Raman spectroscopy was used to examine the structure of the fresh and aged carbon supports. Raman spectra were recorded *ex situ* using a Renishaw InVia spectrometer with the near-IR line of LASER diode (785 nm). The Raman photons were collected on a Peltier-cooled CCD detector and the spectral resolution was about 1 cm^{-1}. The measurements were performed with a ×50 LF objective and the LASER power was about 0.2 mW on the sample. For the sake of comparison, the Raman spectra were normalized to the intensity of the peak at ~1350 cm^{-1}, which corresponds to the band of the disordered graphitic lattice-surface layer edge. For Raman spectroscopy measurements, 40 µL of catalyst ink have been deposited on the glassy carbon support in order to avoid a support contribution, according to the procedure detailed in [8].

X-ray photoelectron spectroscopy was performed on a XR3E2 spectrometer (Vacuum Generator) baring a Mg Kα (1253.6 eV) X-ray source powered at 300 W (15 kV, 20 mA). The kinetic energy of the photoelectrons was measured using a hemispherical electron analyzer working in the constant pass energy mode (30.0 eV). The analysis chamber was kept below 10^{-9} to 10^{-10} mbar background pressure during the data acquisition, which was performed for 0.1 eV increments, at 50 ms dwelling times. The analyses were performed at an angle 90° between the Pt/C sample surface and the analyzer. The charging effect was corrected by referring all the binding energies to the graphene component of the carbon C1s peak at 284.3 eV [8].

3. Results & Discussion

The Characterization and CO-stripping tests performed before and after each AST are shown in Fig.1; the comparison of the ECSA losses is given in Fig.1.g for the three different media. The results show a loss of active surface area for both acidic and alkaline media, with an average value of 57.4, 17.3 and 22.4% of loss, respectively for the NaOH, $HClO_4$ and H_2SO_4 solution. The degradation in alkaline medium is about 3 times worse than for acidic media, while only a slight difference can be observed between the results obtained in $HClO_4$ and H_2SO_4. Using $HClO_4$ and H_2SO_4 solutions enabled to investigate a possible effect of the anion-adsorption strength at the Pt sites (larger for sulfate than for perchlorate anions); the anion adsorption strength explains the potential shift of Pt oxide formation visible between Fig.1.c and Fig.1.e, as previously reported in [15]. H_2SO_4 seems slightly more aggressive than $HClO_4$, in agreement with previous results [16,17].

The modification of the CO-stripping voltammogram after the AST clearly gives additional information; the development of a pre-peak at E = 0.7 V *vs*. RHE upon AST in alkaline medium, associated with a shift of the main peak towards lower potential, are attributed to the agglomeration and growth (via a platinum dissolution/redeposition mechanism, or 3D Ostwald ripening) of the Pt nanoparticles on the carbon support, respectively (Fig.1.b and Fig.2.a-d) [18,19]. In addition, the intensity of peak 2 (on Fig.1.g), corresponding to the hydrogen adsorption on edge atoms of platinum particles, has significantly decreased (relatively to peak 3) for the AST in NaOH in comparison with results obtained for the H_2SO_4 solution; this indicates a smaller amount of edge atom sites and confirms the agglomeration process.

None of these features are visible in Fig.1.d and Fig.1.f, where the CO-stripping voltammograms before and after the AST in the acidic media are nearly unchanged. The high extent of ECSA loss in alkaline medium (60 % *vs*. *ca*. 20 % in acidic media) only happens for much harsher and/or longer degradation protocol and at higher temperature in acidic media [7,20]. This extreme degradation for a somewhat mild AST (25°C, 150 cycles between 0.1 and 1.23 V *vs.* RHE), reveals the aggressiveness of the alkaline medium towards the Pt/C nanoparticles. This parallels the recent findings of Cherevko et al: the "transient" corrosion (*i.e.* that which proceeds when cycling the potential in a CV) of smooth Pt surfaces in alkaline medium starts at lower potential (by *ca*. 50-100 mV) and is *ca*. twice harsher than in acidic medium [10], a last figure which

agrees with the present differences of ECSA loss measured in acidic and alkaline environments. In addition, the extent of agglomeration monitored on the CO-stripping CV is only observed in acidic media in presence of reducing agent such as CO atmosphere [20,21]. ILTEM imaging was performed to shed light on the morphological changes of the Pt/C catalyst and to understand the origin of the ECSA loss differences.

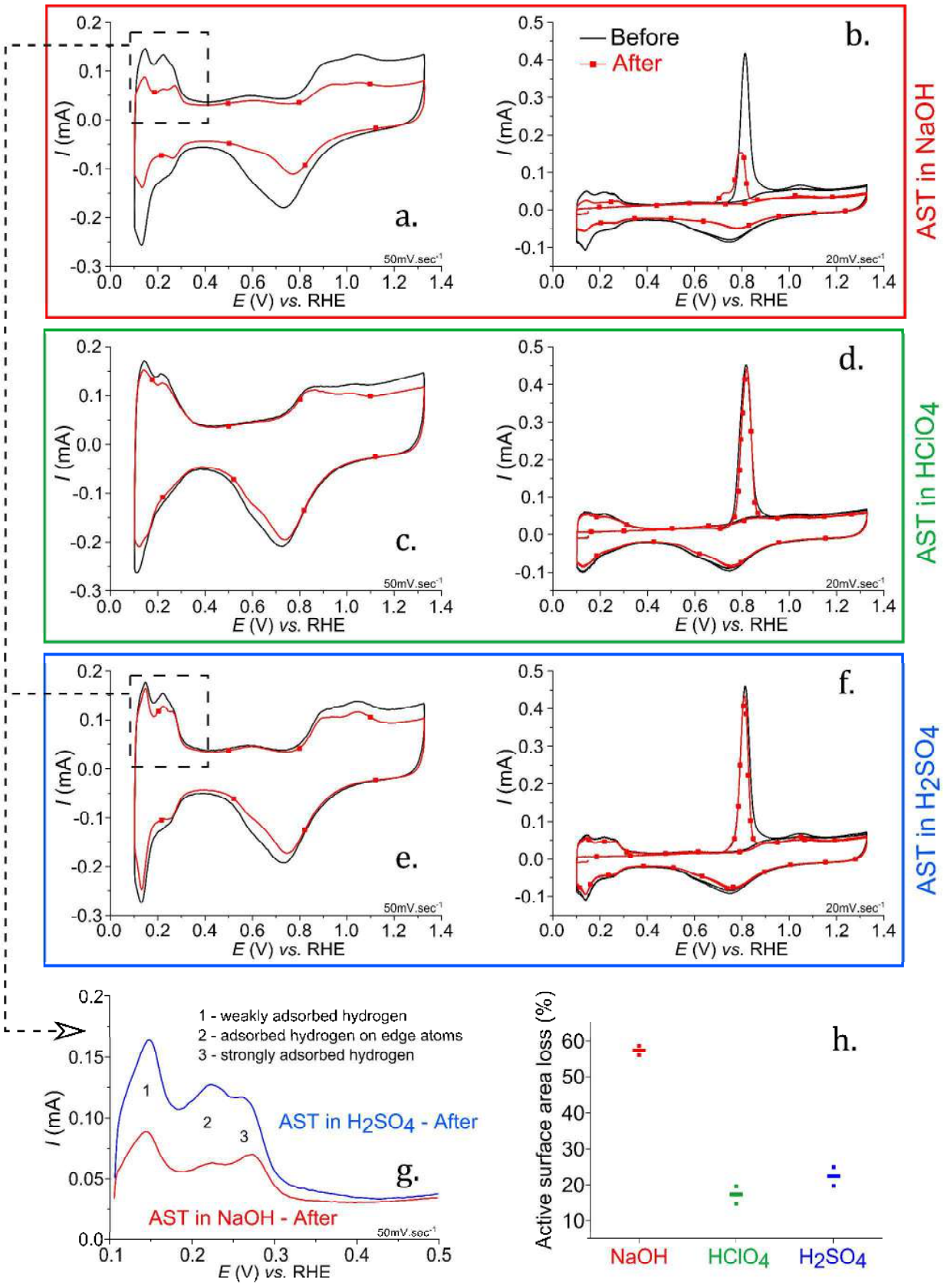

Figure 1 *– Characterization and CO-stripping voltammograms carried out in 0.1 M H_2SO_4 solution at 25°C before/after AST performed in a,b) NaOH c,d) $HClO_4$ or e,f) H_2SO_4. Comparison of characterization voltammograms performed after an AST in NaOH and in H_2SO_4 solutions (g). Corresponding relative active surface area losses for each electrolyte medium (h).*

Fig.2 shows the micrographs obtained before and after the AST in 0.1 M solutions of NaOH, $HClO_4$ and H_2SO_4, and the associated particle size distribution (PSD) histograms.

A slight increase of Pt nanoparticles sizes is observed in acidic media (Fig.2.f and Fig.2.h), due to Pt dissolution/redeposition mechanism, expected for the high/low potential vertex used in the AST [7,20]. It corresponds to a tailing of the PSD towards large nanoparticle sizes at the expense of the smaller nanoparticle sizes, which can sign non-negligible dissolution/redeposition (3D Ostwald ripening) processes [4,22,23]. In alkaline medium, Fig.2.e also indicates a slight increase of the nanoparticles size, but in this case, the PSD histograms essentially flattens: both the amount of very small nanoparticles (between 1 and 2 nm) and of larger nanoparticles slightly increased too; the former could result from the better micrographs contrast after aging in NaOH (the smaller nanoparticles are better visualized then, owing to the sharp decrease of nanoparticles density over the carbon (see below). Moreover, in alkaline medium, the non-negligible agglomeration of the Pt particles evidenced by ILTEM (Fig.2.a-d), explains the shape of the CO-stripping features, with a large CO-electrooxidation pre-peak 0.7 V *vs.* RHE (attributed to the nanoparticles agglomeration [19]).

Whatever the media, particle detachment is evidenced (white markers ease the observation on Fig. 2.d,g,j, being admitted that these markers are by no means quantitative). The absolute number of Pt nanoparticles counted on the ILTEM images before and after the "acidic" AST however demonstrate that the loss of nanoparticles after the AST (10 and 15 % for an AST in H_2SO_4 and $HClO_4$, respectively) is not enough to account for all the ECSA loss (22 and 17 % for an AST in H_2SO_4 and $HClO_4$, respectively). This again shows that the nanoparticle size increase (by Pt dissolution/redeposition) non-negligibly accounts for the active surface area loss electrochemically measured upon acidic AST (see Fig. 1 and Fig.2.f-k). On the contrary, the AST in alkaline medium yields a very large extent of Pt nanoparticles loss (63 %), that matches well with the ECSA loss (57 %). This shows that most of the surface area loss after the "alkaline" AST is due to the simple loss of Pt nanoparticles, and not from quantitative dissolution/redeposition.

As shown in previous works, particles detachment can be linked to both a modification of the chemistry of the carbon support, which changes the interaction between the Pt particles and the support by modifying their anchoring sites on the support, and/or to consequent carbon corrosion in the vicinity of the nanoparticles [7,8,23,24].

Raman spectroscopy measurements have allowed to highlight that such huge degradation in alkaline media cannot be related to severe carbon corrosion, which is a major issue in the acidic environment of a PEMFC for long-term operation [24]. Indeed, four successive degradation tests (250 cycles in 0.1 M NaOH between 0.1 and 1.23 V *vs.* RHE at 100 mV sec^{-1} and 25°C) have been performed and Raman spectroscopy has been carried out on the pristine electrode and after each degradation test. Whereas Fig.3.a clearly illustrates the loss of active surface area in the H_{UPD} and platinum oxides regions (the degradation being more intense during the first part of the degradation protocol, suggesting that the first cycles are the most detrimental), the Raman spectra (Fig.3.b) show no special modification of the intensity of the G-band (1585 cm^{-1}, ideal graphitic lattice) and D1-band (1350 cm^{-1}, disordered graphitic lattice-graphene layer edge) vibrational modes. This indicates that no significant carbon corrosion processes happen until 1000 cycles in these conditions, which obviously rules out any carbon corrosion processes after only 150 cycles in the AST results previously reported in Fig. 1 and Fig. 2.

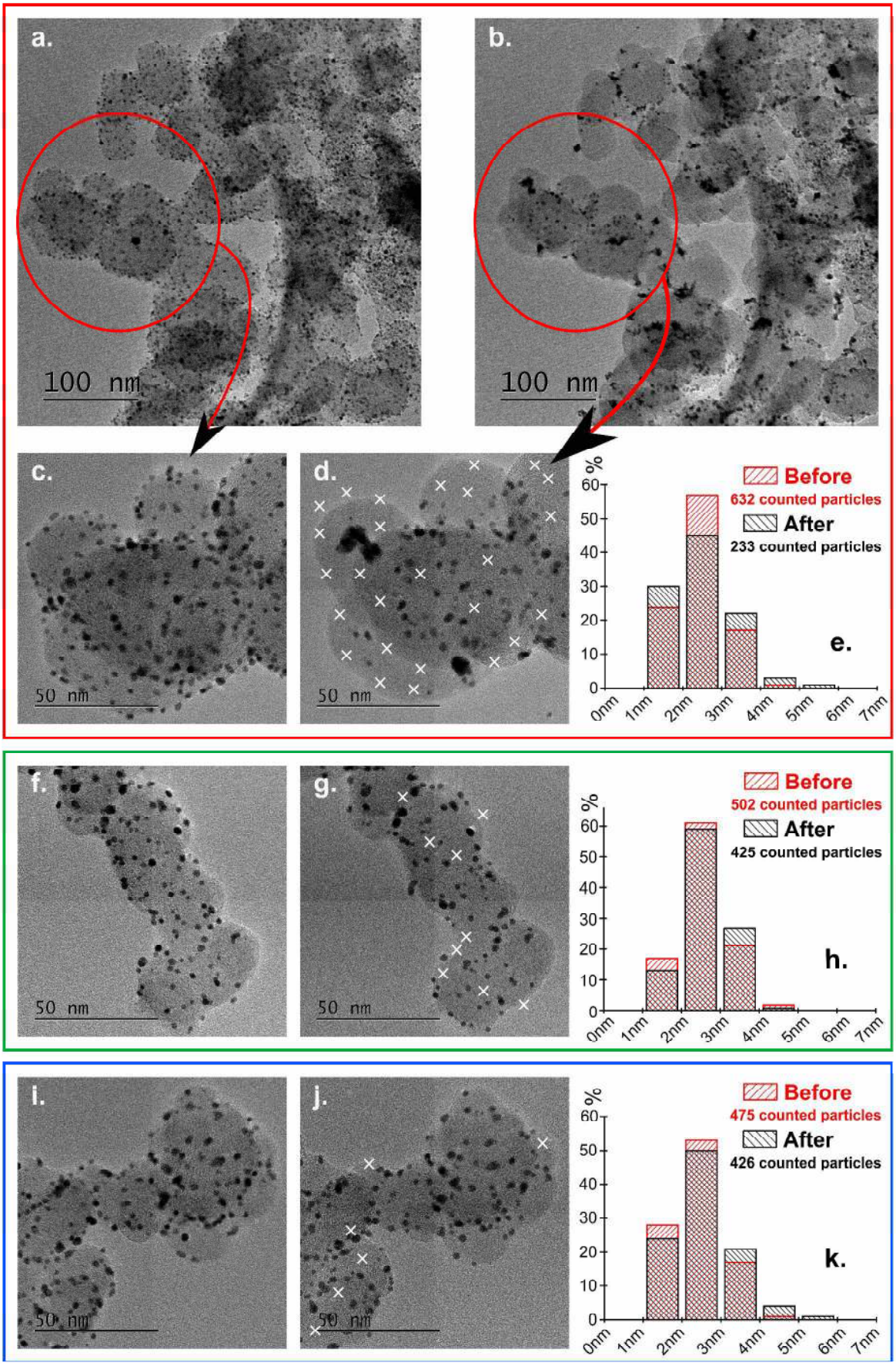
a.
100 nm
b.
100 nm
c.
50 nm
d.
50 nm
Before
632 counted particles
After
233 counted particles
e.
AST in NaOH
f.
50 nm
g.
50 nm
Before
502 counted particles
After
425 counted particles
h.
AST in HClO4
i.
50 nm
j.
50 nm
Before
475 counted particles
After
426 counted particles
k.
AST in H2SO4
%
0nm
1nm
2nm
3nm
4nm
5nm
6nm
7nm

Figure 2 *- ILTEM micrographs pre- and post-AST at 25°C in NaOH (a, b, c, d), $HClO_4$ (f, g) and H_2SO_4 (i, j). The white crosses highlight the nanoparticles loss (in a non-comprehensive manner). Corresponding nanoparticle size distribution histograms in NaOH (e) $HClO_4$ (h) and H_2SO_4 (k). The number of particles counted on the ILTEM images before and after the AST demonstrate the much larger loss of nanoparticles in alkaline medium than in acidic ones.*

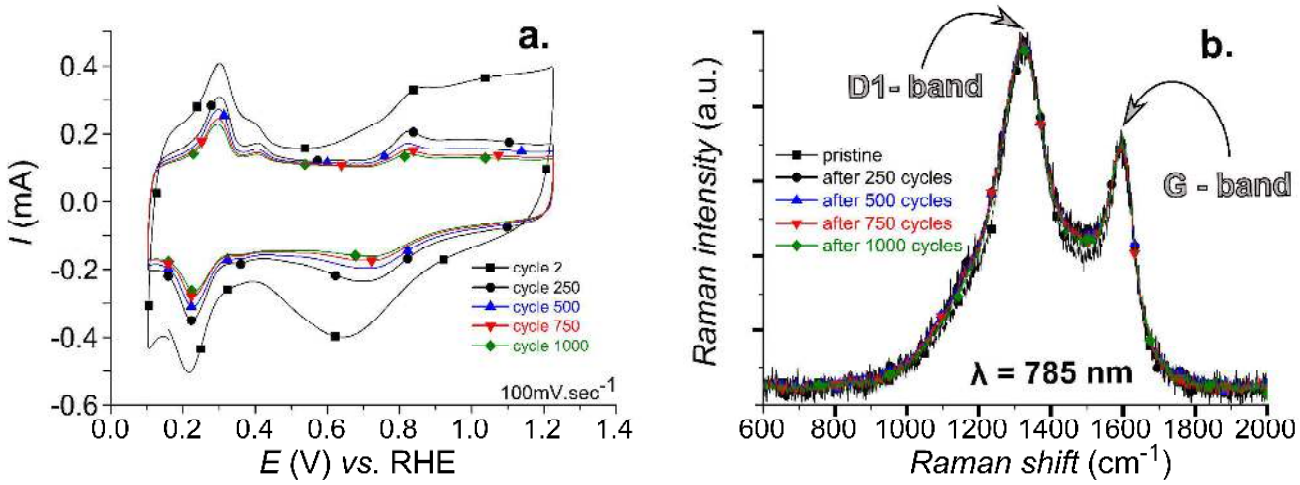

Figure 3 *– Successive AST performed in 0.1 M NaOH at 25°C (a) and Raman spectroscopy results (Normalized) obtained after each AST (b).*

The XPS patterns of the C1s contribution (Fig. 4) also show no sign of severe carbon corrosion after the AST, should it be in alkaline or acidic medium.

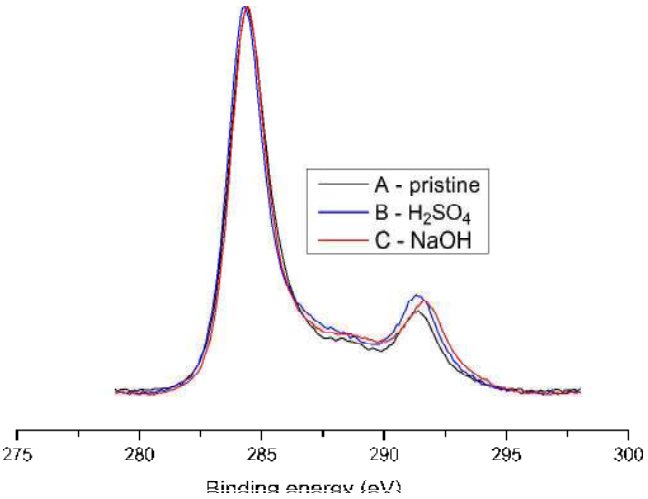

Figure 4 *– XPS data for the Pt/C electrocatalysts in its pristine state and after the AST in 0.1 M H2SO4 and in 0.1 M NaOH.*

Finally, both the XPS and Raman data agree with the electrochemical characterizations (the double layer current hardly varies upon the AST) and the ILTEM images (no signs of severe modification of the carbon shape were observed on Fig.2.a-d), thereby suggesting that the Pt nanoparticles detach from the carbon, simply following the destruction of their anchoring sites to the carbon surface. To the author's opinion, this could follow the subtle modifications of the carbon surface chemistry in the vicinity of the platinum nanoparticle in alkaline medium, but also the harsher "transient" corrosion of the platinum surfaces in alkaline than in acidic medium [10], witnessed by Cherevko et al. for larger potential values (above 1.3 V *vs*. RHE) than in the present work.

4. Conclusion

This work clearly demonstrates that alkaline medium is really more aggressive for Pt/C catalysts than acidic ones for a given accelerated stress test (150 cycles from 0.1 to 1.23 V *vs*. RHE). An impressive loss of ECSA (about 60 %) is only observed upon AST in 0.1 M NaOH, whereas the ECSA loss is limited to *ca.* 20 % in acidic media. In the latter cases, Pt dissolution/redeposition and a low extend of particle detachment have been monitored. On the contrary, the huge degradation observed in alkaline medium (with respect to the extremely small number of cycles performed: 150) follows the very large loss of Pt nanoparticles (*ca*. 63 %). Such particles detachment from the carbon surface is not due to extensive carbon corrosion, as demonstrated by combined ILTEM (no quantitative change of the carbon shape is detected after AST), Raman spectroscopy (no significant modification of D1-band and G-band vibrational modes has been observed even after 1000 cyclic voltammetry cycles) and XPS results (the C1s

band is literally unchanged upon any AST). A modification of the carbon (extreme) surface chemistry in alkaline media, which modifies the anchoring sites of the particles on the support, could explain such degradation; more experiments will be performed to investigate this hypothesis.

AUTHOR INFORMATION

Corresponding Author

* Marian.Chatenet@grenoble-inp.fr; Tel.: +33 476826588; Fax: +33 476826777; (M. Chatenet).

Author Contributions

The manuscript was written through contributions of all authors. / All authors have given approval to the final version of the manuscript. / ‡These authors contributed equally. (match statement to author names with a symbol)

Funding Sources

Region Rhône-Alpes (ARC Energies) supported the research of the manuscript (PhD thesis of Anicet Zadick).

ACKNOWLEDGMENT

The authors thank “la Region Rhône-Alpes (ARC Energies)” for funding this work. This work was performed within the framework of the Centre of Excellence of Multifunctional Architectured Materials "CEMAM" n° AN-10-LABX-44-01. Marian CHATENET thanks the French IUF for its support.

REFERENCES

(1) Vielstich, W.; Lamm, A.; Gasteiger, H. A. Handbook of Fuel Cells; Wiley: Chichester, 2003; Vol. 1-4.
(2) Gasteiger, H. A.; Vielstich, W.; Yokokawa, H. Handbook of Fuel Cells; John Wiley & Sons Ltd: Chichester, 2009; Vol. 5-6.
(3) Guilminot, E.; Corcella, A.; Charlot, F.; Maillard, F.; Chatenet, M. J. Electrochem. Soc. 2007, 154, B96-B105.
(4) Dubau, L.; Maillard, F.; Chatenet, M.; Guetaz, L.; Andre, J.; Rossinot, E. J. Electrochem. Soc. 2010, 157, B1887-B1895.
(5) Ferreira, P. J.; la O', G. J.; Shao-Horn, Y.; Morgan, D.; Makharia, R.; Kocha, S.; Gasteiger, H. A. J. Electrochem. Soc. 2005, 152, A2256-A2271.
(6) Durst, J.; Lamibrac, A.; Charlot, F.; Dillet, J.; Castanheira, L. F.; Maranzana, G.; Dubau, L.; Maillard, F.; Chatenet, M.; Lottin, O. Appl. Catal. B: Environmental 2013, 138-139, 416– 426.
(7) Nikkuni, F.; Ticianelli, E.; Dubau, L.; Chatenet, M. Electrocatal. 2013, 4, 104-116.
(8) Castanheira, L.; Dubau, L.; Mermoux, M.; Berthomé, G.; Caqué, N.; Rossinot, E.; Chatenet, M.; Maillard, F. ACS Catal. 2014, 4, 2258-2267.
(9) Meier, J. C.; Katsounaros, I.; Galeano, C.; Bongard, H. J.; Topalov, A. A.; Kostka, A.; Karschin, A.; Schüth, F.; Mayrhofer, K. J. J. Energy Environ. Sci. 2012, 5, 9319-9330.
(10) Cherevko, S.; Zeradjanin, A. R.; Keeley, G. P.; Mayrhofer, K. J. J. J. Electrochem. Soc. 2014, 161, H822-H830.
(11) Olu, P.-Y.; Bonnefont, A.; Rouhet, M.; Bozdech, S.; Job, N.; Chatenet, M.; Savinova, E. Electrochim. Acta 2015, in press, http://dx.doi.org/10.1016/j.electacta.2015.1002.1158.
(12) Pasqualeti, A. M.; Olu, P. Y.; Chatenet, M.; Lima, F. H. B. ACS Catal. 2015, 5, 2778-2787.
(13) Belén Molina Concha, M.; Chatenet, M.; Lima, F. H. B.; Ticianelli, E. A. Electrochim. Acta 2013, 89, 607-615.
(14) Nikkuni, F. R.; Dubau, L.; Ticianelli, E. A.; Chatenet, M. Appl. Catal. B: Environmental 2015, 176-177, 486-499.
(15) Maillard, F.; Savinova, E.; Simonov, P. A.; Zaikovskii, V. I.; Stimming, U. J. Phys. Chem. B 2004, 108, 17893-17904.
(16) Furuya, Y.; Mashio, T.; Ohma, A.; Tian, M.; Kaveh, F.; Beauchemin, D.; Jerkiewicz, G. ACS Catal. 2015, 5, 2605-2614.
(17) Takahashi, I.; Kocha, S. S. J. Power Sources 2010, 195, 6312-6322.
(18) Maillard, F.; Eikerling, M.; Cherstiouk, O. V.; Schreier, S.; Savinova, E.; Stimming, U. Faraday Discus. 2004, 125, 357-377.
(19) Maillard, F.; Schreier, S.; Hanzlik, M.; Savinova, E. R.; Weinkauf, S.; Stimming, U. Phys. Chem. Chem. Phys. 2005, 7, 385-393.
(20) Dubau, L.; Castanheira, L.; Berthomé, G.; Maillard, F. Electrochim. Acta 2013, 110, 273– 281.
(21) Zhao, Z.; Dubau, L.; Maillard, F. J. Power Sources 2012, 217, 449-458.
(22) Guilminot, E.; Corcella, A.; Chatenet, M.; Maillard, F.; Charlot, F.; Berthome, G.; Iojoiu, C.; Sanchez, J.-Y.; Rossinot, E.; Claude, E. J. Electrochem. Soc. 2007, 154, B1106-B1114.
(23) Shao-Horn, Y.; Sheng, W.; Chen, S.; Ferreira, P.; Holby, E.; Morgan, D. Top. Catal. 2007, 46, 285-305.
(24) Dubau, L.; Castanheira, L.; Maillard, F.; Chatenet, M.; Lottin, O.; Maranzana, G.; Dillet, J.; ElKaddouri, A.; Basu, S.; De Moor, G.; Flandin, L.; Caqué, N. Int. J. Hydrogen Energy 2014, 39 21902-21914.

Insert Table of Contents artwork here